

## Regular article

# Dynamics of the transmembrane domain of the ErbB-2 receptor\*

Jean-Pierre Duneau<sup>1</sup>, Serge Couzry<sup>2</sup>, Yves Chapron<sup>2</sup>, Monique Genest<sup>1</sup>

<sup>1</sup> Centre de Biophysique Moléculaire, UPR 4301 CNRS, affiliated to the University of Orléans, rue Charles Sadron, F-45071 Orleans Cedex 02, France

<sup>2</sup> Département de Biologie Moléculaire et Structurale, CENG, CEA, 17 rue des Martyrs, F-38054 Grenoble Cedex 9, France

Received: 9 May 1998 / Accepted: 3 September 1998 / Published online: 17 December 1998

**Abstract.** The structure and dynamics of the ErbB-2 transmembrane domain have been examined using molecular dynamics techniques both in vacuum and within an explicit hydrated L- $\alpha$ -dilauroyl-phosphatidylethanolamine environment. In-vacuum simulations show that a highly cooperative structural transition occurs frequently within the  $\alpha$ -helical transmembrane domain which converts to local  $\pi$ -helices. We show that the  $\alpha$ -helix alteration does not depend upon the force field or initial side-chain conformations but is intimately related to the sequence. The membrane-like environment does not prevent the structural transition in the helix but slows down the peptide dynamics indicating that the appearance of a  $\pi$ -bulge is not an artifact of the vacuum approximation. The consequences of  $\pi$ -helix formation could be very huge for the ErbB-2 receptor which is involved in numerous human cancers and also for other membrane proteins wherein similar local structures are also observed experimentally.

**Key words:** Molecular dynamics simulations – Transmembrane proteins –  $\pi$ -helix formation –  $\pi$ -bulge

## 1 Introduction

The oncogene products of the family of the epidermal growth factor receptor (EGFR) tyrosine kinase receptors are among the proteins that are most often associated with human carcinomas [1]. For example, the malignancy related to the ErbB-2 oncogene is normally the result of overexpression of the protein at the cell surface. Furthermore, a strong transforming effect is also observed in cultured cells, directly related to specific mutations in the single transmembrane domain

(TM) of the protein [2]. The mutations that replace Val659 by Glu, Gln or Asp constitutively activate the receptor by triggering its dimerization in a specific way. The replacement by Gly, His, Lys, Tyr induce the wild phenotype. This specificity has been successfully assayed to inhibit the transforming abilities of the oncogenic receptor by short transmembrane peptides [3].

A molecular model would be very useful to understand the precise nature of the interactions governing the TM associations. Unfortunately, NMR spectroscopy and X-ray crystallography cannot easily be used to give a high-resolution structure of TM dimers mainly because of their hydrophobic sequence but also because of the difficulties of coping with the membrane environment in experiments. Nevertheless, the helical structure of the ErbB-2 TM segment in a membrane environment has been recently confirmed by polarized Fourier Transform Infrared (FTIR) spectroscopy [4].

Although TM dimer structures are of great biological interest (see Sajot et al. this issue), the structural details of the single helical TM are also of importance since they may modulate the dimerization process.

Our theoretical approach using molecular dynamic (MD) simulations has been successful for this purpose. In this article we give an overview of the main results obtained from in-vacuum simulations along with new data about the dynamics of the ErbB-2 TM embedded within an explicit membrane-like environment. A series of simulations of the transmembrane segment bearing transforming and non-transforming mutations at the specific position 659 have been performed. Our simulations show that a highly reproducible and cooperative transition affects the ErbB-2 helical segment corresponding to conversions between the  $\alpha$ -helical hydrogen bonded structure and the  $\pi$ -helical hydrogen bonded structure. This phenomenon is shown to be independent of the force field, the initial side-chain conformers or the peptide environment.

## 2 Methods

The transmembrane peptides considered in this study comprise the sequence from residues 651 to 679 of the whole ErbB-2 TM protein: L<sup>T</sup>S<sup>I</sup>I<sup>S</sup>A<sup>V</sup>X<sup>G</sup>I<sup>L</sup>L<sup>V</sup>V<sup>V</sup>L<sup>G</sup>V<sup>V</sup>F<sup>G</sup>I<sup>L</sup>I<sup>K</sup>R<sup>R</sup>Q. X denotes

\* Contribution to the Proceedings of Computational Chemistry and the Living World, April 20–24, 1998, Chambéry, France

Correspondence to: M. Genest  
Tel.: +33-2-38 25 76 68; Fax: +33-2-38 63 15 17  
e-mail: geneste@cnrs-orleans.fr

the mutation site at position 659 and is a Val residue in the wild sequence, or a Gly, Glu, Asp or Gln residue in the mutated sequences. The Glu and Asp side chains are considered in the protonated state. Another peptide designed to study the role of the  $\beta$ -branched residues was built by replacing the six remaining Val residues of the Gly mutant by six Ala residues.

For each sequence, the initial canonical  $\alpha$ -helix structure was energy minimized for 200 steps of steepest descent before starting different simulations by varying the initial conditions for atomic velocities, the side-chain conformers and by maintaining, or not maintaining, the first and last terminal helix turns close to the  $\alpha$ -helical structure by smooth distance constraints. The simulations were performed using explicit polar hydrogen atoms and aliphatic hydrogen atoms as united atoms with a relative dielectric constant of 1 without a cutoff distance for van der Waals and electrostatic interactions. All the peptides were globally uncharged. The simulations were carried out using the GROMOS [5] and CHARMM [6] force fields according to the protocols detailed elsewhere [7, 8]. A total of 18 in-vacuum simulations ranging from 500 to 1500 ps were generated to correctly sample the helix dynamics features.

To better approximate the membrane environment the transmembrane peptide was embedded in a hydrated L- $\alpha$ -dilauroylphosphatidyl-ethanolamine (DLPE) bilayer model. Each monolayer was organized into two concentric rings of lipids surrounding the peptide giving rise to a cylindrical-shaped lipid/peptide system including 52 DLPE molecules. This system was immersed into a cylinder of previously equilibrated TIP3 water molecules. Two hydration layers providing a complete hydration of the lipid head groups were obtained after the exclusion of water located between the two planes produced by the lipid carbonyl groups. Water molecules in close contact with the lipids and peptide atoms were also discarded. The all-*trans* configuration of the hydrocarbon tails of the lipids chosen for the construction of the initial system led to a hydrophobic thickness that perfectly match the hydrophobic core of the peptide and head group/water interfaces at the level of the polar residues at each helix extremity. The transmembrane helix/hydrated DLPE system is non-periodical. A cylindrical stochastic potential [9] consisting of a slightly attractive and strongly repulsive part was applied to the lipids and water within a radius of 24 Å from the cylinder axis. We tested these boundary conditions to accommodate a proper area per polar head on both membrane faces that ranged between 41 Å<sup>2</sup> and 49.1 Å<sup>2</sup>, the values for the gel phase and the liquid crystalline phase of pure DLPE respectively [10]. In addition, to avoid the escape of water a similar boundary potential was applied on the two hydration layers to mimic planar boundaries. Such soft boundary conditions reproduced the appropriate lipid/water behaviour [Duneau JP, submitted]. No further control such as lateral pressure was imposed to this simple system which can be viewed as a more realistic environment around the transmembrane peptide and not as a pure lipid bilayer.

The system was then carefully energy minimized in successive runs for several hundred steps of conjugate gradient [11] before the start of the simulations. Two 500 ps production periods were generated after a gradual thermalization to 315 K with an equilibration period of 100 ps at the same temperature.

The 'in-lipids' simulations were performed with X-PLOR [6]. Parameters for the lipids, the peptide and water molecules were taken from the CHARMM force field [12] except the charges for DLPE which were implemented from a semi-empirical calculation using MOPAC/MNDO93. A cutoff value of 11 Å was used for non-bonded interactions with a shifted electrostatic function and a dielectric constant of 1. A smooth switching function over 1 Å was used for van der Waals interactions.

### 3 Results

#### 3.1 Simulations in vacuum

Table 1 gives the different conditions under which the five 1-ns simulations were produced to analyse the

Val659Gly transmembrane peptide behaviour. The main result of this series is that the hydrogen-bond (HB) network of the canonical  $\alpha$ -helix systematically converts to local  $\pi$ -HBs resulting in an altered structure termed a  $\pi$ -bulge, depicted in Fig. 1. These results demonstrate that the observed  $\alpha$ -helix alteration does not depend on helix end constraints or on bond lengths constrained by applying the SHAKE algorithm (simulation G/4). Moreover, initial side-chain conformations with their preferential  $\chi_1$  rotamers in  $\alpha$ -helical structure (set 1) [13], or with  $\chi_1$  rotamers rotated by 120° from these ideal values (set 2), do not prevent the appearance of the  $\alpha/\pi$  transition. Finally, the most important result is that the helix behaviour is similar when using the two force fields (simulation G/5).

Among the 16 1-ns simulations summarized in Table 2, only 3 performed on the oncogenic TM sequences did not reveal the  $\alpha/\pi$  transition. The results show that when the  $\pi$ -deformation is observed it may give rise to an almost complete  $\pi$ -helix of about 20  $\pi$ -HBs as seen in 4 simulations or, more frequently, to a limited  $\pi$ -stretch that covers a large part of the N-terminal side of the peptide as seen in 6 simulations. Three other simulations gave rise to a less-extended deformation considered as an incipient  $\pi$ -helix structure. The initiation time of the transition is, on average, 500 ps.

The different steps of the mechanism of the initiation taking place after the first  $\alpha$ -HB disruption, and the mechanism of elongation of the  $\pi$ -helix structure are detailed in Fig. 2. The initiation is the limiting step for this highly cooperative transition that arises over a sub-picosecond time scale. When the process is started, the  $\pi$ -HB network extends towards the two helix extremities by two different mechanisms. One is very efficient and allows the formation of a new  $\pi$ -HB towards the N-terminus in 10 ps, on average. At this helix side, the interface between the  $\alpha$ - and  $\pi$ -HB networks is achieved by a bifurcated HB. Towards the C-terminus, the elongation takes place more slowly in 100 ps on average. A carbonyl group is excluded from the HB network and this feature is the most drastic structural consequence of the  $\pi$ -bulge formation. It is systematically found at the interface between the  $\alpha$  and  $\pi$ -HB networks and indicates the C-terminal end of the  $\pi$ -helix.

A graphical view of the ErbB-2 TM  $\alpha$ -helix shows that the bulky  $\beta$ -branched residues (Val, Ile, Thr), often in successive arrangement, are also in spatial proximity. It is known that these residues generate unfavourable

**Table 1.** Conditions used to performed the five 1-ns molecular dynamics (MD) simulations on the Val659Gly mutant of the ErbB-2 transmembrane (TM) domain. Two sets of side-chain rotamers were tested (see text). SHAKE algorithm is not applied in Gly simulation (GROMOS)

Simulation	Force field	Helix-end constraints	Side-chain rotamers	$\alpha/\pi$ transition
G/1	GROMOS	No	Set 1	Yes
G/2	GROMOS	Yes	Set 2	Yes
G/3	GROMOS	Yes	Set 1	Yes
G/4	GROMOS*	Yes	Set 1	Yes
G/5	X-PLOR	No	Set 1	Yes

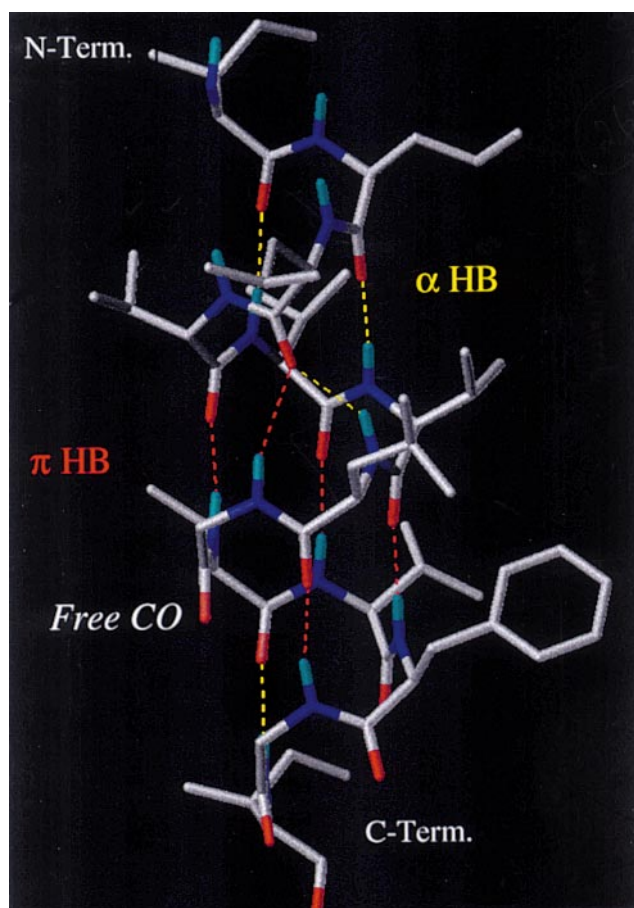


**Fig. 1.**  $\pi$ -bulge within the ErbB-2 TM  $\alpha$ -helix.  $\alpha$ -hydrogen bonds (HBs) are shown in yellow and the 5  $\pi$ -HBs are shown in red. The bifurcated HB at the N-terminal side of the  $\pi$ -deformation and the free CO group excluded from the HB network at the C-terminal side are shown at the junctions of the  $\alpha$ - and  $\pi$ -HB networks. The  $\pi$ -bulge formation induces a rigid body rotation of at least  $100^\circ$  about the helix axis and causes a register shift similar to the deletion of one residue in the sequence

steric interactions within the  $\alpha$ -helix [14] and are presumed to be responsible for helix destabilization. To verify this hypothesis, two additional simulations were performed on a modified sequence of the Val659 Gly mutant, in which the six remaining Val residues were replaced by six Ala residues. These simulations show that the  $\alpha$ -helix is globally maintained except for very short periods during which a short  $\pi$ -deformation occurs transiently at the N-terminal side, where the sequence reveals three  $\beta$ -branched residues (Ile, Thr). These results clearly demonstrate that the intrinsic dynamics of the ErbB-2 TM helix is dominated by the rich  $\beta$ -branched residue sequence. Under vacuum conditions, the  $\alpha$ -helical structure of the ErbB-2 TM appears a metastable conformation.

### 3.2 Simulations in a lipid environment

Although vacuum condition provides a reasonable approximation of the hydrophobic environment of a

**Table 2.** Helix alterations detected at the end of the 16 1-ns MD simulations performed in vacuum for the wild and different mutated ErbB-2 TM sequences. \*: simulation performed with X-PLOR. The time step of the first  $\alpha$ -hydrogen bond (HB) disruption is the initiation time of the  $\alpha/\pi$  transition. The first  $\pi$ -HB and the last  $\pi$ -HB localize the deformation within the helix and indicate the length of the  $\pi$ -stretch. The residue at the specific position 659 is indicated by the one letter code (*G*, *E*, *Q*, *D* or *V*) along with the simulation number.  $\pi$ -HBs are denoted by *i-j* indicating residue *i* of the CO group and residue *j* of the NH group (numbers according to the protein sequence)

Simulations	Initiation step (ps)	First $\pi$ -HB	Last $\pi$ -HB	Number of $\pi$ -HBs
G/1	550	652–657	667–672	16
G/2	700	661–666	667–672	7
G/3	20	653–658	674–679	22
G/4	900	653–658	667–672	15
G/5*	300	654–659	667–672	14
E/1	350	652–657	667–672	16
E/2	–	–	–	0
E/3	550	653–658	667–672	15
Q/1*	550–575*	–	–	0
Q/2*	50	654–659	667–672	14
Q/3*	800	660–665	663–668	4
D/1	300	653–658	673–678	21
D/2	–	–	–	0
D/3	350	653–658	674–679	22
V/1	500	653–658	672–677	20
V/2	100	665–660	658–663	4

transmembrane peptide (especially in the membrane core) [15], differences in the peptide behaviour can exist between vacuum and lipid environments, particularly in regard to the  $\pi$ -helix formation. The important decrease in peptide length (up to 8.5 Å for the formation of the whole  $\pi$ -helix) observed in a few vacuum simulations resulted in a too large membrane thickness variation. Also differences can be expected at the lipid polar head groups/water interfaces particularly in hydrogen bonding interactions.

The effects of the lipidic environment were evaluated on the wild sequence. Although the simple lipid bilayer model used might be questionable and raises the question of the lipid and water behaviour, we verified that the lipid polar groups were correctly hydrated. The radial distribution function of water around the lipid polar head groups, the phosphate oxygens and the carbonyl groups was similar to that calculated from other DLPE membrane models [16–18] and is consistent with experimental data [10]. In addition, we find an electron density profile which has experimental features characteristic of the liquid crystalline phase of the DLPE bilayer [10]. These results [Duneau JP, submitted], which are reasonably successful in reproducing a basic lipid DLPE bilayer, give confidence to the dynamics and structural features of the embedded peptide.

The two 500 ps simulations reveal that, in one case the  $\alpha$ -helix is totally conserved, and in the other case the helix undergoes  $\alpha/\pi$  transitions. Figure 3 gives a view of the initial lipid/water/peptide system and of a snapshot at the end of the 500 ps production period which illustrates the  $\pi$ -deformation. As shown in Table 3, the helix

**Fig. 2.** Details of the  $\alpha/\pi$  transition mechanism: **A** the initiation of the transition occurs when a first  $\alpha$ -HB disrupts (1) leading to the unbounded carbonyl and amide groups; **B** when the following  $\alpha$ -HB is disrupted (2), the first  $\pi$ -type HB may be formed (3) and rapidly a new  $\pi$ -HB appears through a bifurcated HB (4); **C** the smaller  $\pi$ -bulge structure in the  $\alpha$ -helix; **D** the propagation at the C- and N-terminus occur by successively repeating the steps (2), (3) and (4)

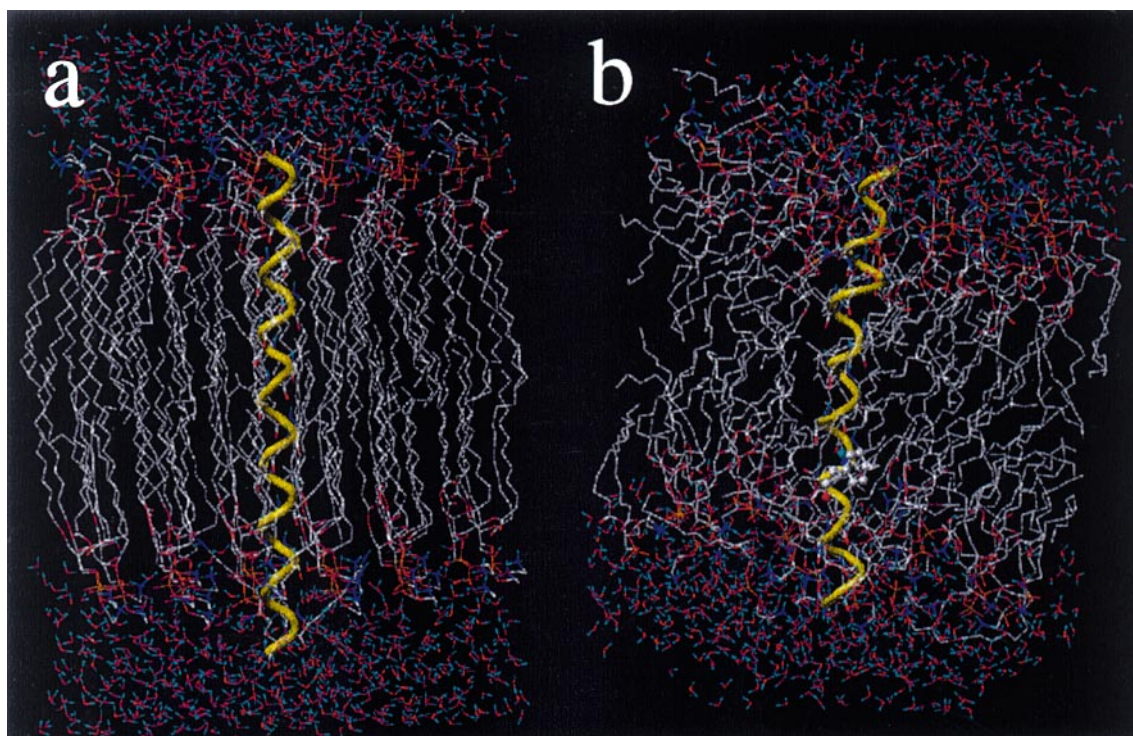
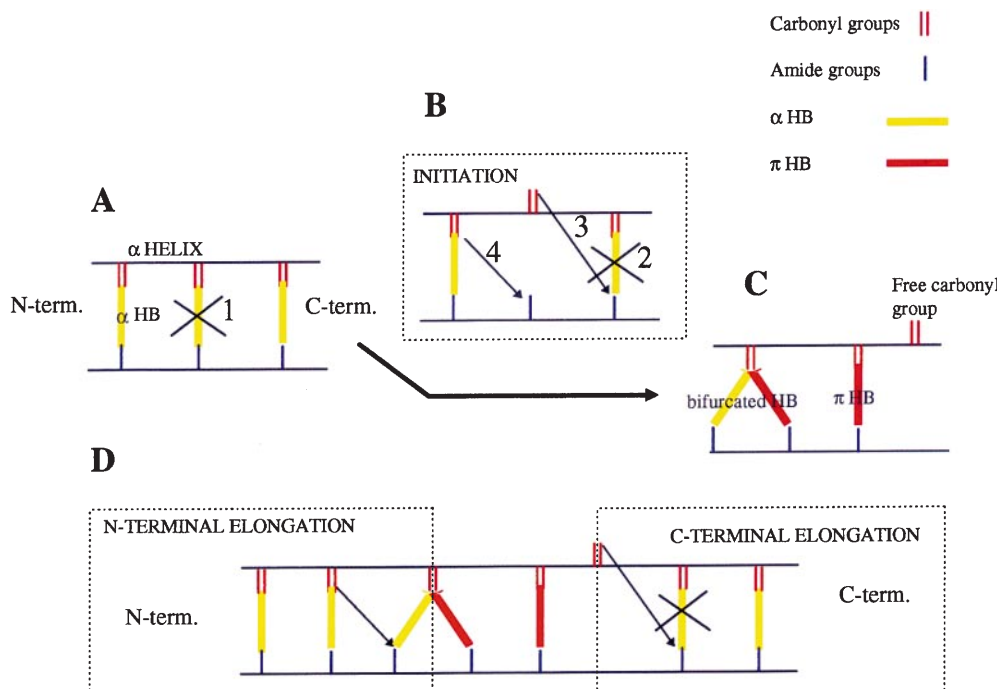


**Fig. 3.** Views of the ErbB-2 TM/DLPE/water system after energy minimization **a** and at the end of the 500 ps dynamics simulation **b**

alteration started during the equilibration period and at the beginning of the production period 2  $\pi$ -HBs are established at the mutation region. The mechanism of the  $\pi$ -elongation observed towards the N-terminal helix is similar to that previously described in vacuum simulations but the time scale of the propagation is slowed

down. A new  $\pi$ -HB formation takes place about 100 ps while it takes about 10 ps in vacuum. The C-terminal propagation is not observed during this 500 ps simulation.

The damping effect due to the lipid proximity is well evidenced by comparing the side-chain motions. Figure 4 shows that the  $\chi_1$  dihedral angle fluctuations observed in vacuum (calculated for simulation G/1) are strongly reduced in the membrane-like environment.

**Table 3.**  $\pi$ -bulge formation in the Val659Gly ErbB-2 TM sequence observed in the 500 ps simulation in membrane-like environment.

Time range for a new $\pi$ -HB formation (ps)	New $\pi$ -HB	Number of $\pi$ -HBs
0*	658–673	2
	657–662	–
25–100	656–671	3
100–300	655–666	4
300–500	654–665	5

\*: the 2  $\pi$ -HBs are formed during the equilibrium period (see text)

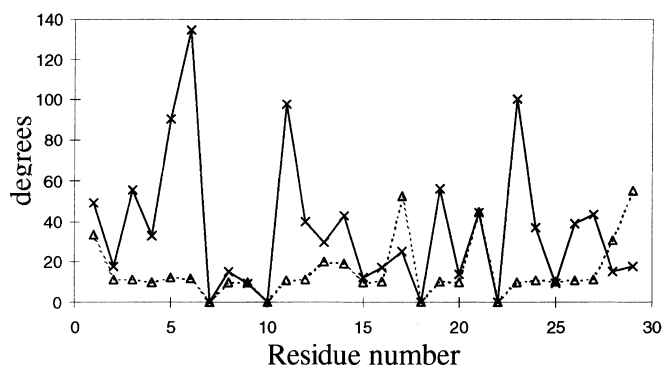


**Fig. 4.** Root mean square values of the  $\chi_1$  dihedral angles calculated for the wild sequence in-vacuum simulation (V/1) (first 500 ps) and in the membrane-like environment

## 4 Conclusion

From 18 1-ns in-vacuum simulations we have shown that the  $\alpha$ -helical structure of the ErbB-2 TM undergoes reproducible conformational transitions resulting in the local replacement of the  $\alpha$ -helix HB pattern by a HB pattern characteristic of a  $\pi$ -helix according to a well-defined mechanism. We have also shown that the dynamics of the ErbB-2 TM is directly related to  $\beta$ -branched residues largely present in the sequence.

The membrane-like model used to approximate the TM environment does not prevent helix alterations. However, although the local  $\pi$ -helix formation seems to be intimately related to its sequence, the membrane environment may also modulate the transition of the transmembrane helix. For example, the thinning of the membrane that accompanies the chain-melting phase transition could be responsible for the early appearance of the  $\alpha/\pi$  transition which is associated with a slight shortening of the helix. Thus, this behaviour can be considered as an illustration of the hydrophobic mismatch effect. Nevertheless, the complete  $\alpha$ -helix may also accommodate the change of the hydrophobic thickness over the 500 ps simulation. Thus it may be inferred that starting simulations from a thermalized membrane environment with disordered lipids (to date, no available data allow the presumption that the liquid crystalline phase is favoured in TM helix contact) would also promote a hydrophobic mismatch and would result in the same TM helix behaviour. Whatever the initial system, 500 ps is a period relatively short to correctly explore the

phase space considering the relaxation of the bilayer and to sample the complex lipid-peptide interactions that control the  $\alpha \rightarrow \pi$  equilibrium of the transmembrane helix. Local  $\pi$ -helix deformations or  $\pi$ -helix elongation may appear over a longer time scale as observed in vacuum simulations [7, 8].

This study, considering the limitation of the model, illustrates the importance of an explicit account of the lipid/water environment in providing a more realistic view of the dynamics of transmembrane helices and conformational changes. In particular, our simulations show that it slows down the time of new  $\pi$ -HB formation and thus their propagation.

Dynamics and structural events might be of great importance in modulation of the receptor activity for which the Val659 Glu mutation in the ErbB-2 TM plays a crucial role in receptor dimer stabilization (Sajot and al. this issue). TM structure heterogeneity such as revealed from MD simulations leads to a rotation of  $100^\circ$  about the helix axis and induces important changes in the distribution of the residues along helix faces, modifying their properties of interactions. Consequently, one can presume that helical structure alterations may play a key role in the dimerization process by optimizing helix-helix interfaces and also by producing drastic conformational changes in the protein. Our findings are supported by the observation of  $\pi$ -helix alterations in membrane proteins of known structure [19] that are now hypothesized to have a functional role.

## References

- Hynes NE, Stern DF (1994) *Biochim Biophys Acta* 1198: 165
- Bargmann CI, Hung MC, Weinberg RA (1986) *Cell* 45: 649
- Lofts FJ, Hurst HC, Sternberg MJ, Gullick WJ (1993) *Oncogene* 8: 2813
- Smith SO, Smith CS, Bormann BJ (1996) *Nature Struct Biol* 3: 252
- van Gunsteren WF (1987) GROMOS, Groningen Molecular Simulation System (BIOMOS) Biomolecular Software b.v. Groningen
- Brunger AT (1992) X-PLOR Manual, A system for crystallography and NMR, Yale University
- Duneau JP, Genest D, Genest M (1996) *J Biomol Struct Dyn* 13: 753
- Duneau JP, Garnier N, Genest M (1997) *J Biomol Struct Dyn* 15: 555
- Brünger A, Brooks CL III, Karplus M (1984) *Chem Phys Letters* 105: 495
- McIntosh TJ, Simon SA (1986) *Biochemistry* 25: 4948
- Powell MJD (1977) *Math Program* 12: 241
- Brooks BR, Brucoleri RE, Olafson BD, States DJ, Swaminathan S, Karplus M (1983) *J Comp Chem* 79: 187
- Dunbrack RL, Karplus M (1993) *J Mol Biol* 230: 543
- Lyu PC, Sherman JC, Chen A, Kallenbach NR (1991) *Proc Natl Acad Sci USA* 88: 5317
- Kaltashov IA, Fenselau C (1997) *Proteins: Struct Func Genet* 27: 165
- Huang P, Perez JJ, Loew GH (1994) *J Biomol Struct Dyn* 11: 927
- Tu K, Tobias DJ, Blasie JK, Klein ML (1996) *Biophys J* 70: 595
- Damodaran KV, Merz KMJ, Gaber BP (1992) *Biochemistry* 31: 7656
- Rajashankar KR, Ramakumar S (1996) *Protein Sci* 5: 932